Dalton Transactions

Cite this: *Dalton Trans.*, 2011, **40**, 1387

www.rsc.org/dalton

PAPER

[1,2,3]Triazolo[1,5-*a*]pyridyl phosphines reflecting the influence of phosphorus lone pair orientation on spectroscopic properties†

Rafael Ballesteros-Garrido,[a] Laurence Bonnafoux,[a] Fernando Blanco,*[c] Rafael Ballesteros,*[b] Frédéric R. Leroux,*[a] Belén Abarca,*[b] Françoise Colobert,*[a] Ibon Alkorta[d] and José Elguero[d]

Received 7th September 2010, Accepted 12th November 2010
DOI: 10.1039/c0dt01183e

A series of new triazolopyridine-based phosphines has been prepared. These compounds revealed unexpected spectroscopic patterns. In particular, the NMR spectra are highly dependent on the relative conformational preference of the phosphine substituent at C7. Here, we report on their complete NMR analysis, X-ray structures and DFT calculations that confirm the particular arrangement of the phosphorus lone pair orbital related to the substituent pattern of the chosen phosphine.

Introduction

Nowadays, an immense number of tertiary phosphines and their transition-metal complexes are known which reflects their importance in homogeneous catalysis. The steric and electronic properties at phosphorus have been often modified in order to fine-tune the efficiency of the transition-metal catalyst.[1] The ligand-binding properties of the phosphines are based on an available lone pair orbital, whereas the steric environment as well as the electronic effect of the phosphorus substituents clearly influences the binding situation. The NMR coupling pattern[2] of phosphine-derivatives is conditioned by the relative orientation of the phosphorus lone pair and the substituents. This phenomenon has been previously studied. For instance Quin *et al.*[3,4] reported on the influence of the lone pair orientation on the ^2J(P,C) coupling constant in 7-(phosphamethyl)-norbornene (**1a** and **1b**) derivatives (Fig. 1).

Some of us have recently reported on the preparation of the first 3-(2′-pyridyl)triazolopyridine-phosphine derivatives **2** (Fig. 2).[5] We could show that these compounds are in equilibrium[6] between two isomer forms A and B (*i.e.*, the isomerization barrier is generally low) and that the A–B ratio depends primarily on the electronic properties of the substituent at C7. The triazolopyridine ring system was revealed to be a sensitive sensor for the electronic situation at phosphorus. In a continuation of our ongoing studies on triazolopyridines[7] and phosphines derived thereof, we now wanted to study the ability of the triazolopyridine ring to reflect the conformational preferences of the attached phosphorus substituents. However, the ring-chain equilibrium rendered an in-depth NMR structural analysis dealing with rotational effects too complicated.

Therefore, we decided to synthesize a new series of non-isomerizable phosphines (PX_2) of 3-methyl-[1,2,3]triazolo [1,5-*a*]pyridine (**3a**), [1,2,3]triazolo[1,5-*a*]pyridine (**3b**), and 3-phenyl-[1,2,3]triazolo[1,5-*a*]pyridine (**3c**) (Fig. 3), and to perform an experimental and theoretical investigation on the influence of phosphorus lone pair orientation on the spectroscopic properties. We will show, how the structural and electronic properties of the phosphine substituent (X) determines both the degree of electron density of the phosphorus lone pair as well as its relative orientation to the triazolopyridine ring, having a significant influence on the NMR spectroscopic patterns.

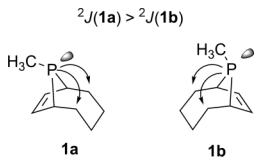

Fig. 1 Influence of the lone pair orientation on the ^2J coupling constant in tertiary phosphines.

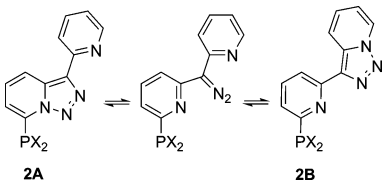

Fig. 2 First triazolopyridine-phosphine ligands.

[a]*Laboratoire de stéréochimie (UMR7509), CNRS-Université de Strasbourg (ECPM), 25 rue Becquerel, 67087, Strasbourg, France. E-mail: frederic.leroux@unistra.fr, francoise.colobert@unistra.fr; Fax: +33 3.68.85.27.42*
[b]*Departamento de Química Orgánica Facultad de Farmacia, Universidad de Valencia Avda. Vicente Andrés Estellés s/n, 46100, Burjassot, Valencia, Spain. E-mail: belen.abarca@uv.es*
[c]*School of Chemistry, University of Dublin, Trinity College, Dublin 2, Ireland. E-mail: blancof@tcd.ie*
[d]*Instituto de Química Médica, CSIC, Juan de la Cierva 3, E-28006, Madrid, Spain*

† Electronic supplementary information (ESI) available: Experimental details, characterization data, as well as X-ray crystallographic data for **4a**, **4b**, **4c**, **5a** and **5b**. CCDC reference numbers 799866–799870. For ESI and crystallographic data in CIF or other electronic format see DOI: 10.1039/c0dt01183e

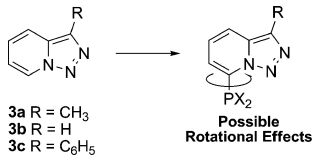

Fig. 3 Target compounds.

Results and discussion

1) Synthesis of triazolopyridine-phosphines

The new triazolopyridine-phosphines were synthesized analogously to the method reported for 7-substituted triazolopyridines. Regioselective metalation[8] of the triazolopyridine ring with butyllithium in toluene at –40 °C, followed by the trapping of the 7-lithio-derivative with the corresponding diphenyl-, dicyclohexyl-, or di-*iso*-propyl-phosphine chloride afforded the desired phosphines **4–6** (Scheme 1). After purification by column chromatography, compounds **4–6** were obtained in moderate yields in almost all cases, except for **6c** which was obtained in a low 23% yield. All the phosphines were revealed to be insensitive towards air and moisture.

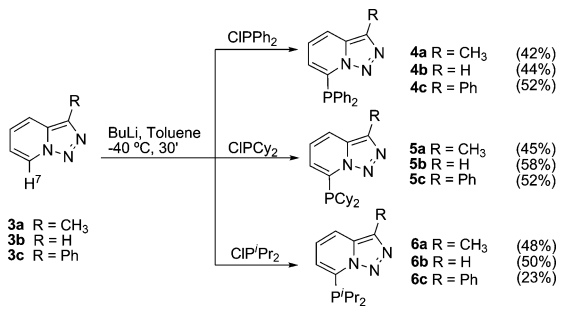

Scheme 1 Preparation of the triazolopyridine-phosphine family.

2) ^{1}H-NMR study of compounds 4–6a–c

The typical ^{1}H-NMR chemical shifts and coupling constants for hydrogen at C4, C5, C6 and C7, which can be found in [1,2,3]triazolo[1,5-*a*]pyridines **3a–c**, are summarized in Fig. 4.[9]

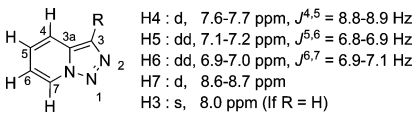

Fig. 4 ^{1}H-NMR chemical shifts and *J* constants for compounds **3a**, **3b** and **3c**.

The analysis of the ^{1}H-NMR spectra of the newly prepared triazolopyridine-phosphine series **4–6** revealed some interesting features. The most significant one is the influence of the substituent at phosphorus on the ^{1}H-NMR signal corresponding to H6. Depending on their nature (phenyl phosphines **4(a–c)** or alkyl phosphines (X = Cy, ^{i}Pr) **5(a–c)** and **6(a–c)**) and, thus, on their electronic and/or steric properties, different trends can be observed.

In diaryl phosphines **4a–c**, the signal corresponding to proton H6 is significantly shifted upfield (δ = 6.37 ppm in **4a**, 6.32 ppm in **4b** and 6.45 ppm in **4c**) compared to 6.9–7.0 ppm in [1,2,3]triazolo[1,5-*a*]pyridine **3b** (Fig. 5).

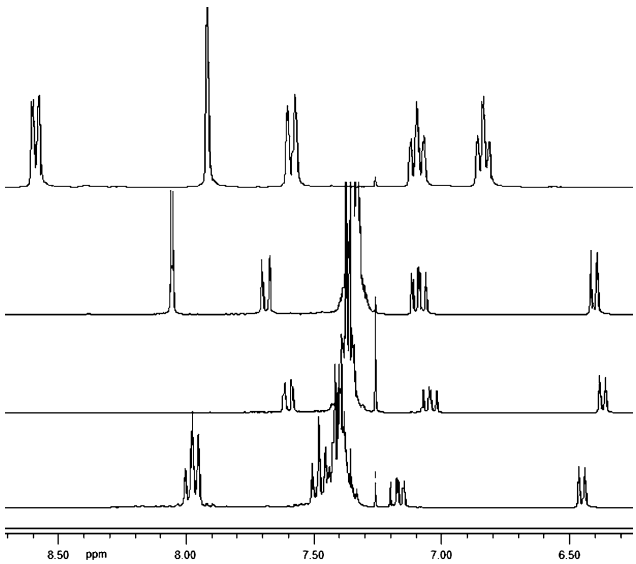

Fig. 5 ^{1}H-NMR comparison (from up to down **3b**, **4a**, **4b** and **4c**), NMR assignation for **3b**: (from left to right: H7, H3, H4, H5 and H6).

In contrast, in dicyclohexyl- (**5a–c**) and di-*iso*-propyl-phosphines (**6a–c**), the signal for H6 is shifted downfield and overlaps with the signal corresponding to H5, forming a multiplet at 7.10–7.20 ppm (Fig. 6).

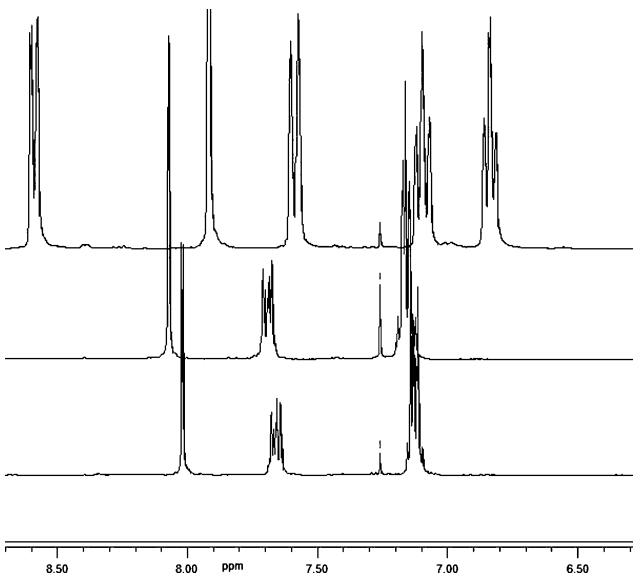

Fig. 6 ^{1}H-NMR comparison (from up to down **3b**, **5b** and **6b**), NMR assignation for **3b**: (from left to right: H7, H3, H4, H5 and H6).

We assumed that the differences in the relative orientation of the substituents X and the lone pair orbital of the phosphine groups in **5** and **6** compared to **4** could explain our observations. In order to confirm this hypothesis, single crystal X-ray analyses and DFT calculations were performed.

3) Single crystal X-ray analysis

Suitable single crystals of triazolopyridine phosphines for X-ray analysis were obtained by slow diffusion of *iso*-propanol into chloroform.

As predicted, triazolopyridine-phosphines adopt different conformations in the solid state. X-Ray analyses of diaryl phosphines **4a–c** (Fig. 7) reveal a spatial arrangement where the phosphorus lone pair is almost in the plane of the triazopyridine ring, oriented towards the triazole system with one of the phenyl groups located above and the other one below the ring (Fig. 9). On the other hand, in alkyl systems, the lone pair remains in the plane of the triazolopyridine ring but pointing to the opposite side near H6 (Fig. 8).

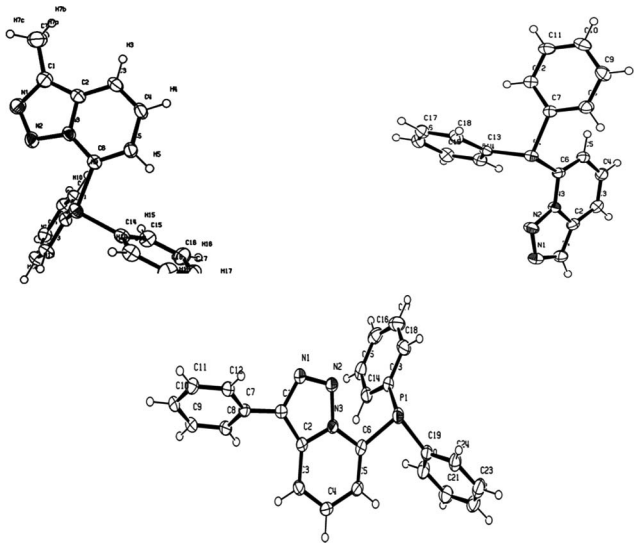

Fig. 7 X-Ray structures for compounds **4a** (up left), **4b** (up right) and **4c** (down).

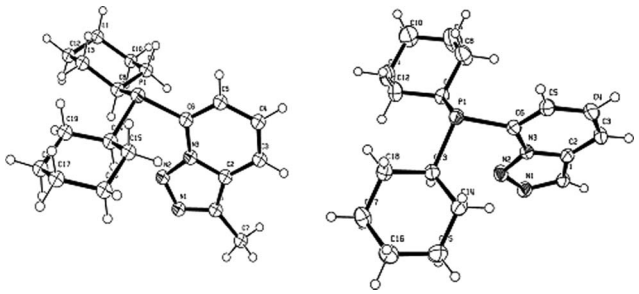

Fig. 8 Molecular structures for compounds **5a** (left) and **5b** (right) in the solid state (X-ray diffraction).

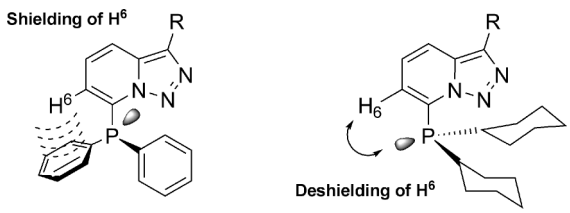

Fig. 9 Different ^{1}HNMR effects depending on the phosphine orientation.

These results encouraged us to further investigate the role of the phosphine orientation, *i.e.* the influence of the relative position of the phosphorus lone pair and the substituents on the ^{1}H-NMR chemical shift of H6. As it was confirmed by single crystal X-ray analysis in diaryl phosphines (**4a–c**) H6 is located in the shielding region of the anisotropic influence of the phenyl rings which explains the observed upfield shift (Fig. 9). This phenomenon has been reported in many cases, the most representative examples being paracyclophanes.[10,11] Contrary, in dialkyl phosphines (**5a–c** and **6a–c**), X-ray analysis shows the phosphorus lone pair pointing towards H6 (Fig. 9), which could be related with the significant H6 downfield shift observed in these compounds.

Thus, single crystal X-ray analysis of **4–6** confirmed that the relative position of the phosphine group in the solid state is not the same for dialkyl and diaryl phosphine derivatives. Opposite effects on the ^{1}H-NMR spectra suggest that for each kind of phosphorus substituent a preferential conformation in solution results. In order to confirm our assumption, a theoretical rotational study was performed.

4) DFT conformational study[12]

Significant effects on the H6 chemical shift observed in the ^{1}H-NMR spectra suggested a preferential conformation of the phosphorus substituent PX_2 depending on the nature of the substituent X. Fig. 10 shows the general formula for the two conformers used in the theoretical study based on the two different geometries found in the X-ray analysis: the conformer **A**, detected in dialkyl substituted phosphines (X = Cy: **5a–c** and ^{i}Pr: **6a–c**) and the conformer **B**, detected in the phenyl series (X = Ph: **4a–c**).

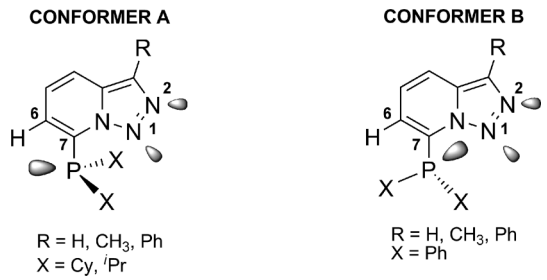

Fig. 10 Preferred conformations of the phosphorus substituent according to the rotational study.

a) Rotational profile. As a first approach we analyzed the rotation of the phosphine group over the triazolopyridine system by IRC (Intrinsic Reaction Coordinate) calculations. In order to simplify the model and minimize the steric factor, we screened the rotation in three phosphines substituted by small groups with different electronic properties: *e*-donor (X = H, CH_3) and *e*-acceptor (X = F). As shown in Fig. 11, starting from the minimum corresponding to the conformer **A**, through the transition states TS $\mathbf{AB_1}$ or TS $\mathbf{AB_2}$, the rotation in either direction lead to two equivalent minima $\mathbf{B_1}$ and $\mathbf{B_2}$ (with substituents located on the opposite side of the ring). The transition between $\mathbf{B_1}$ and $\mathbf{B_2}$ goes through the transition state TS $\mathbf{B_1B_2}$ that presents the lone pair orbital of N1 and the lone pair at phosphorus in the same plane and in a close proximity. Thus, the repulsive effects between both lone pairs could play a determining role in the stability of this structure. This particular role of the phosphorus lone pair in the

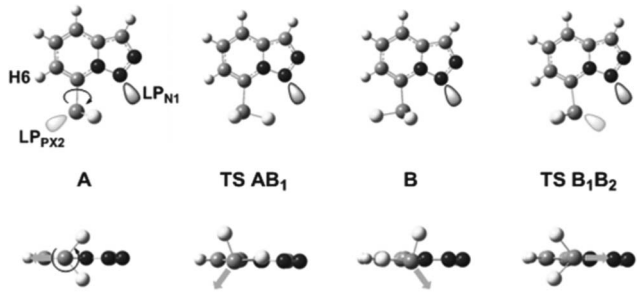

Fig. 11 Two views of rotational mechanism from **A** to **B** (R = H; X = F). Arrows show the orientation of the phosphorus lone pair for each case.

molecular geometry, has already been the subject of numerous studies in organometallics and in organic chemistry in the past, being named the gauche effect.[13]

Fig. 12 shows the reaction path for the studied derivatives in terms of relative energy with respect to the minimum A. For each case the profile is characteristic. Transition barriers found were smaller than 30 kJ mol^{-1}, suggesting that in all cases a free rotation exists. Consequently, the conformational preference can be explained based on a thermodynamic approach. Concerning the electronic nature of the substituents, there are clear differences in the rotational profile when the phosphine is substituted by an *e*-attracting group (X = F) or by an *e*-donor one (X = H, CH_3).

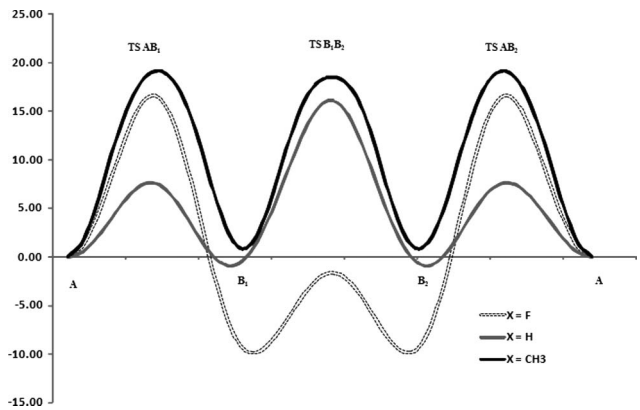

Fig. 12 Reaction path for the studied derivatives (kJ mol^{-1}).

As shown in Fig. 12, when X = F the absolute minimum corresponds to the conformer **B**, with an energy difference to **A** close to 10 kJ mol^{-1}. The orientation of one of the fluorine atoms toward H6 (possible stabilizing interactions) and the low repulsion between the N1- and the phosphine lone pair orbitals (as a consequence of the low electron density of the phosphorus lone pair due to the electron-attracting effect exerted by fluorine), could explain the better stability of this conformation. Moreover, in the conformation **A**, two fluorine atoms are located very close to the N1 lone pair creating a clearly destabilizing situation by electronic repulsion.

For X = H and X = CH_3, however, the energy differences between the conformers **A** and **B** are very low, although in the case of X = CH_3 the conformer **A** is slightly favoured. In this case there are no obvious electronic or steric factors favouring one of the two conformations.

Table 1 Theoretical and experimental ratio of the conformers A/B (see Fig. 10)

X	Compound	ΔE (kJ mol^{-1})	Theoretical	Experimental
Cy	**5b**	–7.5	A	A
^{i}Pr	**6b**	–7.4	A	A
CH_3		–0.8	A/B	
H		0.9	B/B	
Ph	**4b**	8.1	B	B
F		9.9	B	
Br		11.1	B	

A more detailed study including the analysis of the transition states suggests interesting conclusions concerning the influence of the phosphine lone pair in the rotational equilibrium:

– TS **AB$_1$**/TS **AB$_2$**, correspond to the geometry where the phosphine substituents (-F, -H or -CH_3) are close to N1. For X = F and CH_3 the relative energy of this transition state is significantly high (18.0–20.0 kJ mol^{-1}), as a result of the repulsion between N1 and the X substituent. In contrast, this barrier decreases for X = H (7.50 kJ mol^{-1}) as a result of the decrease of repulsion and the possible extra stabilizing interaction by hydrogen bonding (N1–H).

– TS **B$_1$B$_2$** shows similar energetic barriers for X = H and CH_3 (15.00–20.00 kJ mol^{-1}), while it visibly decreases for X = F. In this case, the most decisive factor is the interaction of the phosphorus lone pair and N1. For X = F the effect of the electron-attracting properties of fluorine reduces the electron density of the phosphorus lone pair, decreasing the repulsion with the lone pair at N1. Oppositely, for X = H and CH_3, this repulsive interaction would be increased due to the donor character of the substituents that increase the electronic density of the phosphorus lone pair.

b) Conformational A–B ratios. Subsequently to the rotational study, we performed a conformational analysis of the triazolopyridine-phosphine system as a function of the properties of the phosphine substituent (X). As shown in Table 1, we selected 7 different groups, the experimentally studied (-PPh_2: **4b**, -PCy_2: **5b**, and -P^{i}Pr$_2$: **6b**), and the new ones (X = H, CH_3, F and Br), to optimize their geometries and locate the corresponding minima. In the case of substituents with secondary conformations as a result of the internal movement (cyclohexyl or isopropyl groups), some different geometries were minimized. Table 1 shows the relative energies only between the most stable configurations in the respective conformations **A** or **B** for the different substituents considered. Negative values indicate that the conformer **A** is energetically favoured while positive values indicate a better stability of the isomer **B**.

The general trend suggests that the substituents with positive inductive effect (+I) stabilize the conformer **A** (X = Cy, ^{i}Pr, CH_3), whereas substituents with negative inductive effect (–I) stabilize the conformer **B** (X = Br, F, Ph). This observation is in accordance with the experimental results obtained in this work. Moreover, the calculated energy differences between the respective conformers for the compounds **4b**, **5b** and **6b** (above 5 kJ mol^{-1}) are high enough to explain that these compounds are present only as the most stable form in solution and not as an isomeric mixture.

c) Comparison between predicted and experimental NMR chemical shifts. ^{1}H-NMR of compounds **4b**, **5b**, and **6b** were calculated using the GIAO methodology. Table 2 presents the comparison

Table 2 ^{1}H-NMR spectra comparison

Compound	Data	Conf.	H^{3}	H^{4}	H^{5}	H^{6}
5b (X = Cy)	Calc.	**A**	8.08	7.61	6.99	7.27
5b (X = Cy)	Calc.	**B**	8.01	7.50	7.01	6.88
5b (X = Cy)	Exp.	**A**$^{assig.}$	8.07	7.7–7.6	7.2–7.1	7.2–7.1
6b (X = ^{i}Pr)	Calc.	**A**	8.10	7.64	7.03	7.34
6b (X = ^{i}Pr)	Calc.	**B**	8.04	7.53	7.06	6.90
6b (X = ^{i}Pr)	Exp.	**A**$^{assig.}$	8.02	7.7–7.6	7.2–7.1	7.2–7.1
4b (X = Ph)	Calc.	**A**	8.03	7.67	7.12	7.61
4b (X = Ph)	Calc.	**B**	7.99	7.53	6.92	6.20
4b (X = Ph)	Exp.	**B**$^{assig.}$	7.98	7.61	7.01	6.32

between experimental and calculated[14] values. In all cases the most relevant data concerns the chemical shift of the proton H6. As it can be seen, for dicyclohexyl phosphine-substituted compound **5b**, and the *iso*-propyl derivative **6b**, the experimental values for H6 (δ = 7.2–7.1 ppm) are closer to the calculated one corresponding to conformer **A** (δ = 7.27 ppm), whereas for the phenyl derivative the chemical shift of H6 (δ = 6.32 ppm) is closer to that calculated for conformer **B** (δ = 6.20 ppm). That is consistent with our previous conformational study. Moreover, considering the other significant ^{1}H-NMR signals, the DFT calculated values can be used as a good approximation.

5) ^{13}C-NMR study of compounds 4–6a–c

As it was shown for ^{1}H-NMR, the relative orientation of the phosphine lone pair and substituents also has a significant influence on the ^{13}C-NMR spectra.[2] It is known that the angle and proximity between the phosphorus lone pair orbital and a corresponding coupled atom provide an enhancement of the coupling constant. Recently, Contreras and Peralta[15] reported on the evolution of the $^{2}J(P,C)$ value for ethyl phosphine, observing a dependence on the C–C–P angle. Gil and Philipsborn also showed the influence of the angle on the coupling constants.[16] However, although many phosphine-based compounds are published every year, the assignment of carbon signals and the phosphorus lone pair effect are usually not reported. Furthermore, the already commented free rotation makes the study of these phenomena difficult. As it was mentioned above, in the case of the systems studied in the present work these effects are clearly observed due to the existence in solution of only the most favourable conformer. Contrary to previous studies with phosphines where the carbon assignation was found to be extremely difficult, in the phosphines **4a–c**, **5a–c** and **6a–c** the carbon signals C7, C6, C5, C4 and C3 can be easily assigned (Table 3).

If we compare the ^{13}C-NMR chemical shifts of the parent compounds **3a** and **3c** with the corresponding phosphines, we can highlight some observations: (1) a downfield shift of almost 15 ppm for the carbon atom C7, (2) a downfield shift of 5–10 ppm for the carbon C6 and (3) no significant influence on the carbons C4 and C5. This pattern is the same for alkyl- and/or aryl-phosphines. The value of C3, on the other hand, is strongly conditioned by the R substituent.

As it can be seen, alkyl phosphines (**5a–c** and **6a–c**) show a J(C–P) coupling for carbons C7, C6 and C5 of the triazolopyridyl ring. In contrast, aryl phosphines (**4a–c**) show J(C–P) coupling only for C7 and C3 (Fig. 13). Furthermore, for compounds **4a–c**, coupling constants (^{2}J and ^{3}J) can be found with the carbon of the phenyl substituents of the phosphine group.

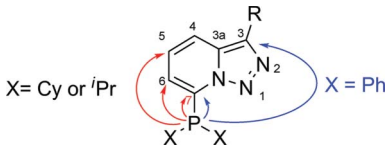

Fig. 13 Selective coupling of different phosphines with the triazolopyridine ring.

We deduce that the relative position of the phosphorus lone pair orbital plays an essential role in the carbon-phosphorus coupling. This phenomenon could be observed due to the relative simplicity of compounds **4a–c** and **6a–c**.

6) Controlling the rotation of aryl phosphines

As outlined before, the dependence of the angle between the phosphorus lone pair and the corresponding carbon atoms must be taken into account in order to analyze the NMR spectra. As we have shown, the same triazolopyridine ring system can have different NMR coupling (P–C) patterns depending on the phosphine type, due to the existence of preferential rotamers.

We were also interested in the possibility to control this angle, by the introduction of large substituents at the 6-position of the triazolopyridine ring. They should increase the steric hindrance and force the aromatic ring of the diphenylphosphino group to turn along the triazolopyridine-phosphine bond. Therefore, we synthesized 6-substituted phosphines starting from

Table 3 ^{13}C-NMR chemical shifts for triazolopyridines **4a–c**, **5a–c** and **6a–c**. C7, C6, C5, C4 and C3 assignation, multiplicity, chemical shift (ppm) and J(P–C) coupling constant (Hz)

Entry	Compound	C7	C6	C5	C4	C3	$^{1}J_{(C7–P)}$	$^{2}J_{(C6–P)}$	$^{3}J_{(C5–P)}$	$^{4}J_{(C3–P)}$
1	**3a**	124.9	115.1	125.1	117.7	133.5	0	0	0	0
2	**3b**[9]	124.7	115.1	125.0	117.6	133.3	0	0	0	0
3	**3c**	126.0	115.7	126.1	118.8	131.9	0	0	0	0
4	**4a**	138.4 d	120.9	124.5	117.4	134.2 d	22.4	0	0	1.2
5	**5a**	137.1 d	124.1 d	124.6 d	118.2	134.2	41.8	25.9	8.2	0
6	**6a**	137.5 d	124.2 d	124.2 d	118.1	134.4	42.2	24.2	7.6	0
7	**4b**	138.5 d	120.9	124.5	117.2	125.6 d	22	0	0	1.6
8	**5b**	136.7 d	122.5 d	124.5 d	117.8	125.7	41.8	26.7	8.5	0
9	**6b**	137.4 d	122.7 d	124.4 d	117.9	125.6	41.8	26.1	8.3	0
10	**4c**	139.3 d	120.9	124.9	117.9	137.8 d	23.3	0	0	1.9
11	**5c**	137.6 d	125.1 d	124.6 d	118.8	137.8	44.2	27.6	8.7	0
12	**6c**	138.2 d	124.6 d	124.7 d	118.8	137.9	43.6	26.2	8.3	0

3-methyl-6-bromo-[1,2,3]triazolo[1,5-*a*]pyridine (**7**),[17] by regioselective metalation with LDA followed by trapping with diphenylphosphine chloride. In this way, compound **8** was obtained in 57% yield (Scheme 2).

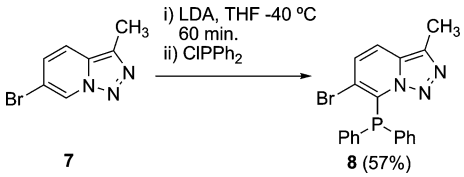

Scheme 2 Synthesis of compound **8**.

Analysis of the ^{13}C-NMR spectra now revealed P–C coupling constants with C7, C6, C5 and C3a. This kind of coupling has previously not been observed with diaryl phosphines and can therefore be taken as confirmation of our hypothesis (Fig. 14).

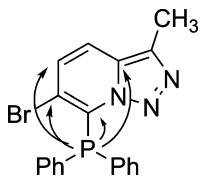

Fig. 14 ^{13}C-NMR coupling pattern of compound **8**.

According to the ^{13}C-NMR spectrum, the phosphorus lone pair orbital should be perpendicular to the triazolopyridine ring to allow the coupling with C6, C5 and C3a. This orientation seems to be reasonable if one considers the interaction between the bromine atom and the phenyl ring. The bond rotation (triazolopyridine-PPh_2) is the only way to minimize steric interaction moving the lone pair from the right side (close to the nitrogen atoms) towards the P/C7/C4 based molecular plane perpendicular to that of the pyridine ring. It is interesting to note that the presence of the bromine atom induces a significant shift in the ^{31}P-NMR of **8** (δ = –2.0 ppm) compared to the parent compounds **4a–c** (δ = –15.4, –15.0 and –14.6 ppm, respectively) probably due to both electronic and steric effects.

Conclusion

In summary, we have reported the preparation of non-isomerizable triazolopyridine-phosphines and we have highlighted their spectroscopic (NMR) properties. By means of DFT calculations, X-ray and NMR analysis we have been able to show and predict how the phosphine orientation can influence the NMR pattern. We have also pointed out how its relative position is dependent on the phosphine substituent, but also on the steric hindrance (Fig. 15).

The orientation of the phosphorus lone pair induces an uncommon ^{13}C-NMR coupling pattern. This phenomenon was clearly identified due to the simplicity of compounds **4–6(a–c)** and **8**. The lone pair has been found to favour P–C NMR coupling constants when the carbon atoms are near to, coplanar to, or on the same side as it.

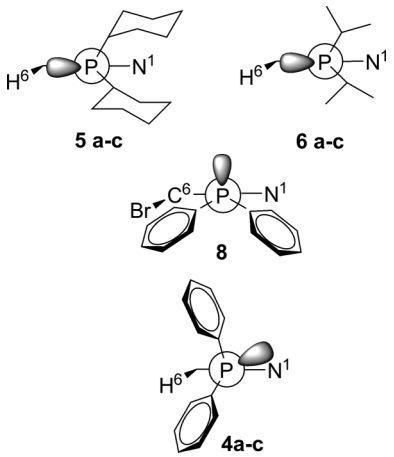

Fig. 15 Lone pair relative position upon different substrates.

Experimental section

General methods

Starting materials, if commercial, were purchased and used as such, provided that adequate checks (melting ranges, refractive indices, and gas chromatography) had confirmed the claimed purity. When known compounds had to be prepared according to literature procedures, pertinent references are given. Air- and moisture-sensitive materials were stored in Schlenk tubes. They were protected by and handled under an atmosphere of argon, using appropriate glassware. Tetrahydrofuran was dried by distillation from sodium after the characteristic blue colour of sodium diphenyl ketyl (benzophenone-sodium "radical-anion") had been found to persist. Ethereal or other organic extracts were dried by washing with brine and then by storage over sodium sulfate. Melting ranges (M.p.) given were determined on a Kofler heated stage and found to be reproducible after recrystallization, unless stated otherwise ("decomp."), and are uncorrected. If melting points are missing, it means all attempts to crystallize the liquid at temperatures down to –75 °C failed. Column chromatography was carried out on a column packed with silica-gel 60 N spherical neutral size 63–210 µm. ^{1}H and (^{1}H decoupled) ^{13}C nuclear magnetic resonance (NMR) spectra were recorded at 400 or 300 and 101 or 75 MHz, respectively. Chemical shifts are reported in δ units, parts per million (ppm) and were measured relative to the signals for residual chloroform (7.27 ppm). Coupling constants J are given in Hz. Coupling patterns are abbreviated as, for example, s (singlet), d (doublet), t (triplet), q (quartet), quint (quintet), sp (septuplet), td (triplet of doublets), m (multiplet), app. s (apparent singlet) and br (broad).

General protocol: synthesis of [1,2,3]triazolo[1,5-*a*]pyridine based monophosphines

At –40 °C, butyllithium (1 eq) in hexane (1.54 M) was added dropwise to a solution of the corresponding 3-substituted[1,2,3]triazolo[1,5-*a*]pyridine (1 eq) in toluene. After 0.5 h, a solution of chlorophosphine (1 eq) in toluene was added dropwise. After 1 h, the solution was allowed to reach room temperature. Water was added, followed by extraction with

dichloromethane. The combined organic layers were dried over sodium sulfate, filtered, and evaporated.

7-(Diphenylphosphino)-3-methyl-[1,2,3]triazolo[1,5-*a*]pyridine (4a). Starting from 3-methyl-[1,2,3]triazolo[1,5-*a*] pyridine (**3a**, 1.0 g, 7.5 mmol) in toluene (50 mL). The crude product was purified by filtration on silicagel to afford 7-(diphenylphosphino)-3-methyl-[1,2,3]triazolo[1,5-*a*]pyridine (**4a**; 1.0 g, 42%) as a colorless solid. mp 142–144 °C. – ^{1}H NMR (300 MHz, $CDCl_3$): δ = 7.60 (d, J = 8.8 Hz, 1 H, H4), 7.45–7.30 (m, 10 H, PPh_2), 7.05 (dd, J = 8.8, 6.9 Hz, 1 H, H5), 6.37 (d, J = 6.8 Hz, 1 H, H6), 2.62 (s, 3 H, CH_3). – ^{13}C NMR (75 MHz, $CDCl_3$): δ = 138.4 (d, J = 22 Hz, C7) 134.5 (d, J = 1.2 Hz, 1 C, C3), 134.2 (d, J = 21 Hz, 4 CH, *o*-Ph), 132.6 (d, J = 8,3 Hz, 2 C, *ipso*-Ph), 131.3 (s, 1 C, C3a), 129.7 (s, 2 CH, *p*-Ph), 128.84 (d, J = 7.7 Hz, 4 CH, *m*-Ph), 123.1 (s, CH, C5), 120.8 (s, CH, C6), 117.2 (s, CH, C4), 10.5 (s, CH_3). – ^{31}P NMR (161 MHz, $CDCl_3$): δ = –15.4. – MS (EI): m/z(%) = 317.1 (63) [M^+], 288 (100) [$M^+ - N_2$], 212.1 (39) [$M^+ - N_2 - Ph$], 183.1 (93). – HRMS for $C_{19}H_{17}N_3P$: calcd. 318.1155; found 318.1145.

7-(Diphenylphosphine)-[1,2,3]triazolo[1,5-*a*]pyridine (4b). Starting from [1,2,3]triazolo[1,5-*a*]pyridine (**3b**, 0.4 g, 3.4 mmol) in toluene (17 mL). The crude product was purified by filtration on silicagel to afford 7-(diphenylphosphine)-[1,2,3]triazolo[1,5-*a*]pyridine (**4b**, 0.5 g, 44%) as a colorless solid. mp 160–162 °C. – ^{1}H NMR (300 MHz, $CDCl_3$): δ = 7.98 (d, J = 2.4 Hz, 1 H, H3), 7.61 (d, J = 8.8 Hz, 1 H, H4), 7.30–7.21 (m, 10 H, PPh_2), 7.01 (dd, J = 8.8, 6.9 Hz, 1 H, H5), 6.32 (d, J = 6.8 Hz, 1 H, H6). – ^{13}C NMR (75 MHz, $CDCl_3$): δ = 138.5 (d, J = 22.4 Hz, 1 C, C7) 133.9 (d, J = 21.1 Hz, 4 CH, *o*-Ph), 133.2 (s, 1 C, C3a), 132.3 (d, J = 8.2 Hz, 2 CH, *ipso*-Ph), 129.6 (s, 2 CH, *p*-Ph) 128.7 (d, J = 7.8 Hz, 4 CH, *m*-Ph), 125.6 (d, J = 1.6 Hz, 1 C, C3), 124.5 (s, 1 CH, C5), 120.8 (s, 1 CH, C6), 117.2 (s, 1 CH, C4). – ^{31}P NMR (161 MHz, $CDCl_3$): δ = –15.0. – MS (EI): m/z(%) = 303.1 (78) [M^+], 275.1 (10) [$M^+ - N_2$], 274.1 (55) [$M^+ - N_2 - H$], 198.1 (23) [$M^+ - N_2 - Ph$], 183.1 (93). – HRMS for $C_{18}H_{14}N_3P$: [M+H^+] calcd. 304.0998; found 304.0969.

7-(Diphenylphosphino)-3-phenyl-[1,2,3]triazolo[1,5-*a*] pyridine (4c). Starting from 3-phenyl-[1,2,3]triazolo[1,5-*a*] pyridine (**3c**, 0.4 g, 2.1 mmol) in toluene (14 mL). The crude product was purified by filtration on silicagel to afford 7-(diphenylphosphine)-[1,2,3]triazolo[1,5-*a*]pyridine (**4c**; 1.1 g, 52%) as a yellow oil. – ^{1}H NMR (300 MHz, $CDCl_3$): 7.98 (m, 3 H, H4 + 3-*o*-Ph), 7.52–7.33 (m, 13 H, PPh_2 + 3-*m*-Ph + 3-*p*-Ph), 7.17 (dd, J = 8.8, 6.9 Hz, 1 H, H5), 6.45 (d, J = 6.9 Hz, 1 H, H6). – ^{13}C NMR (75 MHz, $CDCl_3$): δ = 139.3 (d, J = 23.3 Hz, 1 C, C7), 137.8 (d, J = 1.9 Hz, 1 C, C3), 134.2 (d, J = 21.2 Hz, 4 CH, P(*o*-Ph)$_2$), 132.4 (d, J = 8.3 Hz, 2 C, *ipso*-PPh_2), 131.6 (s, 1 C, C3a), 130.2 (s, C, 3-*ipso*-Ph), 129.8 (s, 2 C, P(*p*-Ph)$_2$), 128.9 (d, J = 7.8 Hz, 4 CH, P(*m*-Ph)$_2$), 128.8 (s, 2 CH. 3-*o*-Ph), 127.7 (s, 1 CH, 3-*p*-Ph), 126.6 (s, 2 CH, 3-*m*-Ph), 124.9 (s, 1 CH, C5), 120.9 (s, 1 CH, C6), 117.9 (s, 1 CH, C4). – ^{31}P NMR (161 MHz, $CDCl_3$): δ = –14.6. – MS (EI): m/z(%) = 379.1 (8) [M^+], 351.1.1 (37) [$M^+ - N_2$], 350.1 (20) [$M^+ - N_2 - H$], 185.1 (72) [P(Ph)$_2$], 183.1 (100). – HRMS for $C_{24}H_{18}N_3P$: [M+O+Li^+] calcd. 402.1343; found 402.1316.

7-(Dicyclohexylphosphino)-3-methyl-[1,2,3]triazolo[1,5-*a*] pyridine (5a). Starting from 3-methyl-[1,2,3]triazolo[1,5-*a*] pyridine (**3a**, 1.0 g, 7.5 mmol) in toluene (50 mL). The crude product was purified by filtration on silicagel to afford 7-(dicyclohexylphosphino)-3-methyl-[1,2,3]triazolo[1,5-*a*] pyridine (**5a**; 1.0 g 45%) as a colorless solid. mp 93–95 °C. – ^{1}H NMR (300 MHz, $CDCl_3$): δ = 7.56 (d, J = 8.2 Hz, 1 H, H4), 7.15–7.00 (m, 2 H, H6 + H5), 2.73–2.57 (m, 2 H, PCy_2), 1.94 (dd, J = 16.5, 8.6 Hz, 2 H, PCy_2), 1.72 (d, J = 7.5 Hz, 2 H, PCy_2), 1.53 (m, 4H, PCy_2), 1.14 (m, 12 H, PCy_2). – ^{13}C NMR (75 MHz, $CDCl_3$): δ = 137.1 (d, J = 41.2 Hz, 1C, C7) 134.2 (s, 1 C, C3), 131.5 (s, 1 C, C3a), 124.1 (d, J = 25.9 Hz, 1 CH, C6), 122.5 (d, J = 9 Hz, 1 CH. C5), 117.8 (s, 1 CH, C4), 32.4 (d, J = 11 Hz, 2 CH, (CH)-PCy_2), 30.9 (d, J = 19 Hz, 2 CH_2, CH_2), 29.9 (d, J = 9 Hz, 2 CH_2, CH_2), 26.7 (d, J = 3.2, Hz, 2 CH_2, CH_2), 26.6 (bs, 2 CH_2, CH_2), 26.2–25.9 (bs, 2 CH_2, CH_2), 10.4 (s, CH_3). – ^{31}P (161 MHz, $CDCl_3$): δ = 6.5. – MS (EI): m/z(%) = 329.2 (35) [M^+], 301.2 (33) [$M^+ - N_2$], 246. (81) [M^+ – Cy], 218.2 (100) [$M^+ - N_2$ – Cy], 137 (66) [$M^+ - N_2$ – 2Cy]. – HRMS for $C_{19}H_{28}N_3P$ [M+Li]: calcd. 336.2176; found 336.2215.

7-(Dicyclohexylphosphino)-[1,2,3]triazolo[1,5-*a*]pyridine (5b). Starting from [1,2,3]triazolo[1,5-*a*]pyridine (**3b**, 0.4 g, 3.4 mmol) in toluene (17 mL). The crude product was purified by filtration on silicagel to afford 7-(dicyclohexylphosphino)-[1,2,3]triazolo[1,5-*a*]pyridine (**5b**; 0.6 g, 58%) as a colorless solid. mp 124–126 °C. – ^{1}H NMR (300 MHz, $CDCl_3$): δ = 8.07 (s, 1 H, H3), 7.73–7.65 (m, 1 H, H4), 7.21–7.10 (m, 2 H, H5 + H6), 2.72–2.55 (m, 2 H, CH-PCy_2), 2.02–1.90 (m, 2 H, CH_2), 1.79–1.70 (m, 2 H, CH_2), 1.63–1.51 (m, 4 H, CH_2), 1.35, 1.16 (m 10 H, CH_2). – ^{13}C NMR (75 MHz, $CDCl_3$): δ = 137.1 (d, J = 41.8 Hz, 1 C, C7), 133.7 (s, 1 C, C3a), 125.6 (s, 1 C, C3), 124.6 (d, J = 25.9 Hz, 1 CH, C6), 124.1(d, J = 8.2 Hz, 1 CH, C5), 118.2 (s, 1 CH, C4), 32.6 (d, J = 11.3 Hz, 2 CH, (CH)-PCy_2), 30.9 (d, J = 19.1 Hz, 2 CH_2, CH_2), 30.0 (d, J = 9.0 Hz, 2 CH_2, CH_2), 26.7 (d, J = 3.6 Hz, 2 CH_2, CH_2), 26.6 (s, 2 CH_2, CH_2), 26.8 (d, J = 1.1 Hz, 2 CH_2, CH_2). – ^{31}P NMR (161 MHz, $CDCl_3$): δ = 7.0. – MS (EI): m/z(%) = 315.2 (42) [M^+], 287.2 (33) [$M^+ - N_2$], 232.1 (57) [M^+ – Cy], 204.2 (100) [$M^+ - N_2$ – Cy], 151.1 (45) [M^+ – 2Cy + 2H], 123 (25) [$M^+ - N_2$ – 2Cy + 2H]. – HRMS for $C_{18}H_{26}N_3P$ [M + Li]: calcd. 322.2019; found 322.1975.

7-(Dicyclohexylphosphino)-3-phenyl-[1,2,3]triazolo[1,5-*a*] pyridine (5c). Starting from 3-phenyl-[1,2,3]triazolo[1,5-*a*] pyridine (**3c**, 0.3 g, 1.3 mmol) in toluene (25 mL). The crude product was purified by filtration on silicagel to afford 7-(dicyclohexylphosphino)-3-methyl-[1,2,3]triazolo[1,5-*a*] pyridine (**5c**; 0.3 g, 52%) as a colorless solid. mp 93–95 °C. – ^{1}H NMR (300 MHz, $CDCl_3$): δ 8.00 (m, 3 H, H4 + 3-*o*-Ph), 7.51 (J = 7.6, 7.6 Hz, 2 H, 3-*m*-Ph), 7.37 (m, 1 H, 3-*p*-Ph), 7.25–7.20 (m, 2 H, H5 + H6), 2.82–2.60 (m, 2 H, CH-PCy_2), 2.02–1.91 (m, 2 H, CH_2), 1.81–1.70 (m, 3 H, CH_2), 1.63–1.51 (m, 5 H, CH_2), 1.39–1.04 (m 10 H, CH_2). – ^{13}C NMR (75 MHz, $CDCl_3$): δ = 137.8 (s, 1 C, C3), 137.6 (d, J = 44.5 Hz, 1 C, C7), 131.7 (s, 1 C, C3a), 130.7 (s, 1 C, 3-*ipso*-Ph), 128.9 (s, 2 CH, 3-*o*-Ph) 127.7 (s, CH, 3-*p*-Ph), 126.6 (s, 2 CH, 3-*m*-Ph), 125.1 (d, J = 27.6 Hz, 1 CH, C6), 24.6 (d, J = 8.7 Hz, 1 CH, C5), 118.8 (s, 1 CH, C4), 32.7 (d, J = 27.6 Hz, 2 CH, (CH)-PCy_2), 31.1 (d, J = 19.3 Hz, 2 CH_2, CH_2), 30.2 (d, J = 9.0 Hz, 2 CH_2, CH_2), 26.9 (s, 2 CH_2, CH_2), 26.8 (d, J = 3.5 Hz, 2 CH_2, CH_2), 26.7 (s, 2 CH_2, CH_2), 26.2 (s, 2 CH_2, CH_2). – ^{31}P NMR (161 MHz, $CDCl_3$): δ = 6.5. – MS (EI): m/z(%) = 391.2 (25) [M^+], 363.2 (80) [$M^+ - N_2$], 280. (100) [$M^+ - N_2$ –Cy], 199.1 (90), 146.1 (90). – HRMS for $C_{24}H_{30}N_3P$ [M + O + Li]: calcd. 414.2280; found. 414.2270.

7-(Di-*iso*-propylphosphino)-3-methyl-[1,2,3]triazolo[1,5-*a*] pyridine (6a). Starting from 3-methyl-[1,2,3]triazolo[1,5-*a*] pyridine (**3a**, 1 g, 7.5 mmol) in toluene (17 mL). The crude product was purified by filtration on silicagel to afford 7-(di-*iso*-propylphosphino)-3-methyl-[1,2,3]triazolo[1,5-*a*]pyridine (**6a**, 0.9 g, 48%) as a brown oil. – ^{1}H NMR (300 MHz, $CDCl_3$): δ = 7.60 (d, J = 8.6 Hz, 1 H, H4), 7.21–7.06 (m, 2 H, H5 + H6), 2.97–2.78 (m, 2 H, P(C*H*$(CH_3)_2)_2$), 2.61 (s, 3 H, 3-CH_3), 1.21 (dd, J = 16.1, 7.0 Hz, 6 H, P(CH(C*H*$_3)_2)_2$), 0.88 (dd, J = 13.2, 7.0 Hz, 6 H, P(CH(C*H*$_3)_2)_2$). – ^{13}C NMR (75 MHz, $CDCl_3$): δ = 137.4 (d, J = 41.8 Hz, C7), 134.4 (s, 1 C, C3a), 131.6 (s, 1 C, C3), 124.4 (d, J = 26.1 Hz, 1 CH, C6), 122.7 (d, J = 8.3 Hz, 1 CH, C6), 117.9 (s, 1 CH, C4), 22.6 (d, J = 10.4 Hz, 2 CH, P(*C*H$(CH_3)_2)_2$), 20.7 5 (d, J = 14.5 Hz, 2 CH_3, P(CH(*C*H$_3)_2)_2$), 20,5 (d, J = 4.6 Hz, 2 CH_3, P(CH(*C*H$_3)_2)_2$), 10.4 (s, 3-CH_3). – ^{31}P NMR (161 MHz, $CDCl_3$): δ = 16.1. – MS (EI): m/z(%) = 249.2 (56) [M^+], 221.2 (11) [$M^+ - N_2$], 206.1 (26) [M^+ – ^{i}Prop], 178.1 (100) [$M^+ - N_2$ – ^{i}Prop], 136.1 (64) [$M^+ - N_2$ – 2Cy]. – HRMS for $C_{13}H_{20}N_3P$ [M+Li]: calcd. 256.1550; found 256.1519.

7-(Di-*iso*-propylphosphino)-[1,2,3]triazolo[1,5-*a*]pyridine (6b). Starting from [1,2,3]triazolo[1,5-*a*]pyridine (**3b**, 0.4 g, 3.4 mmol) in toluene (17 mL). The crude product was purified by filtration on silicagel to afford 7-(di-*iso*-propylphosphino)-[1,2,3]triazolo[1,5-*a*]pyridine (**6b**; 0.4 g, 50%) as a brown oil. – ^{1}H NMR (300 MHz, $CDCl_3$): δ = 8.02 (d, J = 8.9 Hz, 1 H, H3), 7.71–7.62 (m, 1 H, H4), 7.17–7.09 (m, 2 H, H5 + H6), 2.77 (m, 2 H, P(C*H*$(CH_3)_2)_2$), 1.13 (dd, J = 15.9, 7.0 Hz, 6 H, P(CH(C*H*$_3)_2)_2$), 0.81 (dd, J = 13.4, 7.0 Hz, 6 H, P(CH(C*H*$_3)_2)_2$). – ^{13}C NMR (75 MHz, $CDCl_3$): δ = 137.5 (d, J = 42.2 Hz, 1 C, C7) 133.6 (s, 1 C, C3a), 125.6 (s, 1 C, C3), 124.3 (d, J = 24.2 Hz, 1 CH, C6), 124.2 (d, J = 7,6.7 Hz, 1 CH, C5), 118.1 (s, 1 CH, C4), 22.5 (d, J = 10.9 Hz, 2 CH, P(*C*H$(CH_3)_2)_2$), 20.4 (d, J = 10.0 Hz, 2 CH_3, P(CH(*C*H$_3)_2)_2$), 20.2 (s, 2 CH_3, P(CH(*C*H$_3)_2)_2$). – ^{31}P NMR (161 MHz, $CDCl_3$): δ = 15.4. – MS (EI): m/z(%) = 235.2 (49) [M^+], 207.2 (21) [$M^+ - N_2$], 192.1 (100) [M^+ – ^{i}Prop], 164.1 (39) [$M^+ - N_2$ – ^{i}Prop], 149.1 (85) [M^+– 2^{i}Prop], 122.1 (42) [$M^+ - N_2$ – 2^{i}Prop + H]. – HRMS for $C_{12}H_{18}N_3P$ [M + Li]: calcd. 242.1393; found 242.1371.

7-(Di-*iso*-propylphosphino)-3-phenyl-[1,2,3]triazolo[1,5-*a*] pyridine (6c). Starting from 3-phenyl-[1,2,3]triazolo[1,5-*a*] pyridine (**3c**, 0.4 g, 2.1 mmol) in toluene (14 mL). The crude product was purified by filtration on silicagel to afford 7-(di-*iso*-propylphosphino)-3-phenyl-[1,2,3]triazolo[1,5-*a*]pyridine (**6c**; 0.3 g, 23%) as a brown oil. – ^{1}H NMR (300 MHz, $CDCl_3$): δ = 7.95–7.85 (m, 3 H, H4 + 3-*o*-Ph), 7.46–7.39 (m, 2 H, 3-*m*-Ph), 7.34–7.26 (m, 1 H, 3-*p*-Ph), 7.19–7.13 (m, 2 H, H5 + H6), 2.85 (m, 2 H, P(C*H*$(CH_3)_2)_2$), 1.17 (dd, J = 16.1, 7.0 Hz, 6 H, P(CH(C*H*$_3)_2)_2$), 0.84 (dd, J = 13.5, 7.0 Hz, 6 H, P(CH(C*H*$_3)_2)_2$). – ^{13}C NMR (75 MHz, $CDCl_3$): δ = 138.2 (d, J = 43.6 Hz, 1 C, C7), 137.9 (s, 1 C, 3-*ipso*-Ph), 131.6 (s, 1 C, C3a), 130.6 (s, 1 C, C3), 128.9 (s, 2 CH, 3-*o*-Ph), 127.8 (s, 1 CH, 3-*p*-Ph), 126.7 (s, 2 CH, 3-*m*-Ph), 124.7 (d, J = 26.2 Hz, 1 CH, C6), 124.6 (d, J = 8.3 Hz, 1 CH, C5), 118.8 (s, 1 CH, C4), 22.8 (d, J = 10.7 Hz, 2 CH, P(*C*H$(CH_3)_2)_2$), 20.7 (d, J = 7. 9 Hz, 2 CH_3, P(CH(*C*H$_3)_2)_2$), 20.5 (d, J = 1.7 Hz, 2 CH_3, P(CH(*C*H$_3)_2)_2$). – ^{31}P NMR (161 MHz, $CDCl_3$): δ = 17.3. – MS (EI): m/z(%) = 311.2 (28) [M^+], 283.2 (58) [$M^+ - N_2$], 240.1 (55) [$M^+ - N_2$ – ^{i}Prop], 198.1 (100) [HM$^+$–N_2 – 2^{i}Prop], 167.1 (51) [$M^+ - N_2$ – 2^{i}Prop + H]. – HRMS for $C_{18}H_{22}N_3P$ [M+Li]: calcd. 318.1716; found 318.1721.

7-(Diphenylphosphino)-6-bromo-3-methyl-[1,2,3]triazolo [1,5-*a*]pyridine (8). At 0 °C butyllithium (18.2 mmol, 11.6 mL, 1.3 eq) in hexanes (1.56 M) was added to a solution of di-*iso*-propylamine (18.2 mmol, 2.6 mL, 1.3 eq) in tetrahydrofuran (150 mL). Then it was cooled to –40 °C and added to a stirred solution of 6-bromo-3-methyl-[1,2,3]triazolo[1,5-*a*]pyridine (**7**; 3.0 g, 14.1 mmol, 1.0 eq) in tetrahydrofuran (150 mL) at –40 °C. The mixture was kept at –40 °C for one hour before diphenylphosphine chloride (0.9 g, 42 mmol, 1.3 eq) in tetrahydrofuran (5 mL) was added. After 1 h, the solution was allowed to reach room temperature. Water (20.0 mL) was added, followed by extraction with dichloromethane (3 × 20.0 mL). The combined organic layers were dried over sodium sulfate, filtered, and evaporated. The crude product was purified by chromatography on silicagel (ethyl acetate/cyclohexane 1 : 4) to afford 7-(diphenylphosphino)-6-bromo-3-methyl-[1,2,3]triazolo[1,5-*a*]pyridine (**8**; 3.2 g. 57%) as a yellow oil. – ^{1}H NMR (300 MHz, $CDCl_3$): 7.49–7.40 (m, 4H), 7.24 (d, J = 9.22 Hz, 1H, H4), 7.18–7.08 (m, 7H), 2.32 (s, 3H, CH_3). – ^{13}C NMR (75 MHz, $CDCl_3$): δ = 135.4 (s, C, C3), 133.9 (d, J = 47.30 Hz, 1 C, C7), 133.3 (d, J = 21.17 Hz, 4 CH, *o*-Ph), 132.3 (d, J = 10.17 Hz, 2 C, *ipso*-Ph), 130.62 (d, J = 1.5 Hz, C, C3a), 129.25 (s, 2 CH, *p*-Ph), 128.64 (d, J = 3.00 Hz, CH, C5), 128.50 (d, J = 6.96 Hz, 4 CH, *m*-Ph), 123.71 (d, J = 34.04 Hz, C, C6), 119.18 (s, CH, C4), 26.99 (s, CH_3). ^{31}P NMR (161 MHz, $CDCl_3$): δ = –2.0. – MS (EI): m/z(%) = 397.1 (25) [M^+], 368.0 (60) [$M^+ - N_2$], 288.1 (80) [$M^+ - N_2$ – Br], 183.1 (100). – HRMS for $C_{19}H_{15}{}^{79}BrN_3P$: [M + H] calcd. 396.0265 found 396.0261. $C_{19}H_{15}{}^{81}BrN_3P$: [M + H] calcd. 398.0245 found 398.0241.

DFT conformational study on isomerism

Geometries of the minima were fully optimised at the B3LYP theoretical level with the 6-31G** basis set as implemented in the Gaussian 03 program.[12] Harmonic frequency calculations verified the nature of the stationary points as minima (all real frequencies). The scanning of the rotation was performed using the IRC type calculation implemented in the Gaussian 03 program at the same level. ^{1}H shieldings of compounds have been calculated over the fully optimized geometries within the GIAO[14] (Gauge-Independent Atomic Orbital) approximation.

X-ray structure determination

CCDC 799866 (**4a**), 799867 (**4b**), 799868 (**4c**), 799869 (**5a**) and 799870 (**5b**) contain the supplementary crystallographic data for this paper.†

Acknowledgements

We are indebted to Dr Lydia Brelot (Service de Radiocristallographie, University of Strasbourg, France) for her assistance with the single crystal structure elucidation. This work was carried out with financial support from the Ministère de la Recherche (France), from the CNRS (France), from the Ministerio de Educación y Ciencia (Project No. CTQ2007-61901/BQU and CTQ2006-15672-C05-03), and the Comunidad Autónoma de Madrid (Project MADRISOLAR, ref. S-0505/PPQ/0225). Thanks are given to the CTI (CSIC) and CESGA for allocation of computer time. RBG is much indebted to the Ministère de l'Éducation Nationale, de la Recherche et de la Technologie

(France) for a doctoral fellowship. LB thanks LONZA AG (Switzerland) for a PhD grant.

References

1 M. K.-T. Ohkuma, R. Noyori, *Catalytic Asymmetric Synthesis* 2nd ed., Wiley-VCH, New York, 2000; J. M. Brown, *Comprehensive Asymmetric Catalysis*, Springer, Berlin, 1999; R. Noyori, *Asymmetric Catalysis in Organic Synthesis*, Wiley, New York, 1994; W. Tang, X. Zhang, *Chem. Rev.* 2003, **103**, 3029–3069.

2 S. Berger, S Braun, H-O. Kalinowski, *NMR-Spektroskopie von Nicht-metallen. Band 3, 31P-NMR-Spektroskopie.* Georg Thieme Verlag, Stuttgart, 1993.

3 L. D. Quin, K. C. Caster, J. C. Kisalus and K. A. Mesch, *J. Am. Chem. Soc.*, 1984, **106**, 7021–7032.

4 L. D. Quin, M. J. Gallagher, G. T. Cunkle and D. B. Chesnut, *J. Am. Chem. Soc.*, 1980, **102**, 3136–3143.

5 R. Ballesteros-Garrido, L. Bonnafoux, B. Abarca, F. Leroux and F. Colobert, *Dalton Trans.*, 2009, 5068–5070.

6 B. Abarca, I. Alkorta, R. Ballesteros, F. Blanco, M. Chadlaoui, J. Elguero and F. Mojarrad, *Org. Biomol. Chem.*, 2005, **3**, 3905–3910.

7 R. Ballesteros-Garrido, F. Blanco, R. Ballesteros, F. R. Leroux, B. Abarca, F. Colobert, I. Alkorta and J. Elguero, *Eur. J. Org. Chem.*, 2009, 5765–5778; R. Ballesteros-Garrido, B. Abarca, R. Ballesteros, C. Ramirez de Arellano, F. R. Leroux, F. Colobert and E. Garcia-Espana, *New J. Chem.*, 2009, **33**, 2102–2106; R. Ballesteros-Garrido, F. R. Leroux, R. Ballesteros, B. Abarca and F. Colobert, *Tetrahedron*, 2009, **65**, 4410–4417; B. Abarca, R. Ballesteros, R. Ballesteros-Garrido, F. Colobert and F. R. Leroux, *Tetrahedron*, 2007, **63**, 10479–10485.

8 B. Abarca, R. Ballesteros, F. Mojarred, G. Jones and D. J. Mouat, *J. Chem. Soc., Perkin Trans. 1*, 1987, 1865–1868.

9 G. Jones, *Adv. Heterocycl. Chem.*, 1983, **34**, 79–143.

10 A. Agarwal, J. A. Barnes, J. L. Fletcher, M. C. McGlinchey and B. G. Sayer, *Can. J. Chem.*, 1977, **55**, 2575–2581.

11 J. S. Waugh and R. W. Fessenden, *J. Am. Chem. Soc.*, 1957, **79**, 846–849.

12 M. J. Frisch, G. W. Trucks, H. B. Schlegel, G. E. Scuseria, M. A. Robb, J. R. Cheeseman, J. A. Montgomery, T. Vreven, K. N. Kudin, J. C. Burant, J. M. Millam, S. S. Iyengar, J. Tomasi, V. Barone, B. Mennucci, M. Cossi, G. Scalmani, N. Rega, G. A. Petersson, H. Nakatsuji, M. Hada, M. Ehara, K. Toyota, R. Fukuda, J. Hasegawa, M. Ishida, T. Nakajima, Y. Honda, O. Kitao, H. Nakai, M. Klene, X. Li, J. E. Knox, H. P. Hratchian, J. B. Cross, V. Bakken, C. Adamo, J. Jaramillo, R. Gomperts, R. E. Stratmann, O. Yazyev, A. J. Austin, R. Cammi, C. Pomelli, J. W. Ochterski, P. Y. Ayala, K. Morokuma, G. A. Voth, P. Salvador, J. J. Dannenberg, V. G. Zakrzewski, S. Dapprich, A. D. Daniels, M. C. Strain, O. Farkas, D. K. Malick, A. D. Rabuck, K. Raghavachari, J. B. Foresman, J. V. Ortiz, Q. Cui, A. G. Baboul, S. Clifford, J. Cioslowski, B. B. Stefanov, G. Liu, A. Liashenko, P. Piskorz, I. Komaromi, R. L. Martin, D. J. Fox, T. Keith, M. A. Al-Laham, C. Y. Peng, A. Nanayakkara, M. Challacombe, P. M. W. Gill, B. Johnson, W. Chen, M W. Wong, C. Gonzalez, J. A. Pople, *Gaussian-03* ed.; Gaussian Inc.: Wallingford CT, 2003.

13 W. E. Buhro, B. D. Zwick, S. Georgiou, J. P. Hutchinson and J. A. Gladysz, *J. Am. Chem. Soc.*, 1988, **110**, 2427–2439 and references cited therein.

14 GIAO: R. Ditchfield, *Mol. Phys.*, 1974, **27**, 789–807; F. London, *J. Phys. Radium*, 1937, **8**, 397–409.

15 R. H. Contreras and J. E. Peralta, *Prog. Nucl. Magn. Reson. Spectrosc.*, 2000, **37**, 321–425.

16 V. M. S. Gil and W. V. Philipsborn, *Magn. Reson. Chem.*, 1989, **27**, 409–430.

17 B. Abarca, R. Ballesteros, R. Ballesteros-Garrido, F. Colobert and F. R. Leroux, *Tetrahedron*, 2008, **64**, 3794–3801.